General Disclaimer

One or more of the Following Statements may affect this Document

- This document has been reproduced from the best copy furnished by the organizational source. It is being released in the interest of making available as much information as possible.

- This document may contain data, which exceeds the sheet parameters. It was furnished in this condition by the organizational source and is the best copy available.

- This document may contain tone-on-tone or color graphs, charts and/or pictures, which have been reproduced in black and white.

- This document is paginated as submitted by the original source.

- Portions of this document are not fully legible due to the historical nature of some of the material. However, it is the best reproduction available from the original submission.

NASA TECHNICAL MEMORANDUM

NASA TM X-73534

NASA TM X-73534

AN EXPERIMENTAL INVESTIGATION WITH ARTIFICIAL SUNLIGHT OF A SOLAR HOT-WATER HEATER

by Frederick F. Simon
Lewis Research Center
Cleveland, Ohio 44135

TECHNICAL PAPER presented at the
Joint Conference of the International Solar Energy Society and the Solar Energy Society of Canada
Winnipeg, Canada, August 15-20, 1976

ABSTRACT

Thermal performance measurements were made of a commercial solar hot-water heat in a solar simulator. The objective of the test was to determine basic performance characteristics of a traditional type of flat-plate collector, with and without side reflectors (to increase the solar flux).

Due to the fact that collector testing in the solar simulator permits us to control the variables that affect collector performance, it was possible to obtain information on each of the following:

(1) The effect of flow and incidence angle on the efficiency of a flat-plate collector (but only without side reflectors)

(2) Transient performance under flow and nonflow conditions

(3) The effectiveness of reflectors to increase collector efficiency for a zero radiation angle at fluid temperatures required for solar air conditioning

(4) The limits of applicability of a collector efficiency correlation based on the Hottel-Whillier equation

AN EXPERIMENTAL INVESTIGATION WITH ARTIFICIAL SUNLIGHT OF A SOLAR HOT-WATER HEATER

by Frederick F. Simon

Lewis Research Center

SUMMARY

Thermal performance measurements were made of a commercial solar hot-water heat in a solar simulator. The objective of the test was to determine basic performance characteristics of a traditional type of flat-plate collector, with and without side reflectors (to increase the solar flux).

Due to the fact that collector testing in the solar simulator permits us to control the variables that affect collector performance, it was possible to obtain information on each of the following:

(1) The effect of flow and incidence angle on the efficiency of a flat-plate collector (but only without side reflectors)

(2) Transient performance under flow and nonflow conditions

(3) The effectiveness of reflectors to increase collector efficiency for a zero radiation angle at fluid temperatures required for solar air conditioning

(4) The limits of applicability of a collector efficiency correlation based on the Hottel-Whillier equation.

INTRODUCTION

An important step in the creation of advanced technology for more efficient and cost effective solar heating and cooling systems is the test and evaluation of solar energy system components. A key solar system component being studied at NASA-Lewis is the flat-plate collector.

Testing and evaluating flat-plate collectors that show promise for solar cooling applications is done outdoors, and indoors in a solar simulator facility. Testing under controlled conditions with a solar simulator is a very effective way of determining performance characteristics of collectors. The basis for this approach is given in reference 1. This paper reports on the performance characteristics of a particular type of flat-plate collector which is representative of a class of collectors. The collector efficiency was determined as a function of fluid inlet temperature, solar flux level, solar flux incidence angle, and flow

Star category 34

rate by the use of artificial sunlight in an indoor facility having a controlled ambient temperature and wind. An investigation was also made on the use of side reflectors to boost the radiation flux at a zero radiation incidence angle. Use is made of the Hottel-Whillier equations for correlating the steady-state performance data.

COLLECTOR DESCRIPTION

The collector tested was obtained from Beasley Industries in Australia and consists of a copper absorber sheet with four parallel 1/2-inch copper tubes soldered to the sheet. The absorber plate has a selective coating of copper oxide. The collector had 2 glass covers, 2 inches of fiberglass insulation behind the absorber plate and overall dimensions of 24 by 52 inches. The collector without and with side mirror reflectors is shown in figures 1(a) and (b), respectively.

EXPERIMENTAL METHOD

Experimental Facility

A sketch of the solar simulator is presented in figure 2. The primary components are the energy source (solar simulator), the liquid flow loop, and the instrumentation and data acquisition equipment.

The solar simulator gives a radiation output which is nearly collimated (solar beam subtense angle of 10^{o}) and has a spectrum close to that of air-mass 2 sunshine. Details of the solar simulator are given in reference 2. The flow loop consists of storage and expansion tanks, pump, heater, test collector and required piping. A 50/50 weight mixture of ethylene-glycol and water is used in the flow loop. Temperatures are measured with chromel constantan thermocouples. Flow rate is determined with a turbine-type flow meter and this measurement is checked by allowing the fluid to enter a graduated cylinder and timing the volume change with a stop watch. Measurements are recorded on magnetic tape and the information sent to a digital computer for data reduction and computation. See reference 3 for more details on the experimental facility.

Test Procedure

The collector to be tested is mounted on the test stand and positioned so that the radiant flux is normal to or at different angles to the collector. Variation of the incident angle is accomplished by rotating the test stand about the vertical axis. The present tests were run at a tilt angle of 57 degrees and solar incident angles of 0, 41.5, 57.5, and 65.2. The flow rates were adjusted to values corresponding to 5, 10, and 20 pounds per hour per square foot of collector absorber area. Be-

fore the simulator is turned on, the collectors are given time to achieve thermal equilibrium at the inlet temperature chosen (1 hr or more). After thermal equilibrium is established for a given inlet temperature, the simulator is turned on and the desired radiant flux is obtained by adjusting the lamp voltage. After steady-state conditions occurred, usually in 10 to 15 minutes, data is recorded. The radiant flux is then readjusted to a second value at the same collector inlet temperature, steady-state conditions obtained, and data again recorded. The collector inlet temperature is then set to another value, and the procedure repeated.

EXPERIMENTAL RESULTS

The experimental efficiency of the collector was calculated using the following equation:

$$\eta = GC_p(T_0 - T_1)/I_{dr} \tag{1}$$

Where G is defined as the flow rate per unit effective area for solar collection

$$G = \frac{\dot{m}}{A_a} \tag{2}$$

The collector efficiency was determined for nominal flow rates of 5, 10, and 20 lb/hr ft^2, inlet temperatures ranging between 76^o and 237^o F, a simulated solar flux ranging between 71 and 315 Btu/hr ft^2, effective wind speed of 7 mph, and a nominal ambient temperature of 75^o F.

Basic Performance Correlation

The equations of Hottel and Whillier (refs. 4 and 5) are used to express the collector performance. These equations are as follows:

$$\eta = F'\left[\alpha\tau - \frac{U_L(\bar{T}_f - T_a)}{I_{dr}}\right] \tag{3}$$

$$\eta = F_R\left[\alpha\tau - \frac{U_L(T_1 - T_a)}{I_{dr}}\right] \tag{4}$$

Equations (3) and (4) indicate that a correlation of the collector performance data is possible by plotting efficiency versus the temperature difference divided by the radiation flux. There has been some suggestion based on analysis (ref. 6) that this correlation is applicable only for a limited radiation flux range. As a check of the possible limitation of the correlating equations (3) and (4), performance data was

obtained using the solar simulator for a radiation flux range of 70 to 300 Btu/hr ft^2. The correlation for this radiation flux range, a flow rate of 10 lb/hr ft^2, and a zero radiation incident angle is given in figure 3. Figure 3 indicates for the collector tested, the validity of the correlation-approach for a wide range of radiant fluxes.

Another interesting point suggested by figure 3 is the simulator's ability to give a fairly constant spectral response for different power levels. This is seen by the small variation of the efficiency data at the intercept of the correlation. At the correlation intercept, the performance data may be expressed according to equation (4) as:

$$\eta = F_R \alpha \tau \tag{5}$$

Since the absorber coating and glass cover are sensitive to wave length, it is expected that spectral changes in the simulators output could affect the absorptivity (α) of the coating and transmittance (τ) of the glass with a resulting change in the intercept as indicated by equation (5).

Effect of Flow Rate

The correlation shown in figure 3 was also obtained for flow rates of 5 and 20 lb/hr ft^2. All these correlations for a radiation incident angle of zero are shown in figure 4 behave in accordance with equations (3) and (4) and the results of Bliss (ref. 7). The plate efficiency factor (F') and the flow efficiency factor (F_R) increase with an increase in flow rate. Therefore, collector performance data plotted in the manner of equations (3) and (4) should show an increase in the intercept and slope with an increase in flow rate. This effect is noted in figure 4.

Effect of Incidence Angle

The intercepts of the correlations shown in figures 3 and 4 are functions of the solar incidence angle (θ_i). This can be seen by inspection of equations (3) and (4), since the absorptance (α) and the transmittance (τ) are functions of the incidence angle. The experimentally determined values of the intercept were correlated as shown in figures 5(a) and (b). Figure 5(b) shows a linear correlation approach given in reference 8.

Transient Performance

In reference 3, a test and data reduction procedure was given for determining collector heat capacity for the case of liquid flow in the collector. The test procedure consists of recording the outlet fluid

temperature of the collector after the simulator lamps are turned off, for an inlet temperature equal to the ambient temperature and calculating the collector heat capacity with the following equation:

$$C_c = \frac{\left(F'U_L + \frac{GC_p}{K}\right)(t_2 - t_1)}{\ln\left[\frac{T_o(t_1) - T_a}{T_o(t_2) - T_a}\right]} \tag{6}$$

where

$$K = \frac{GC_p}{F'U_L}\left(\frac{F'}{F_R} - 1\right) \approx \frac{1}{2}$$

The equation for the collector heat capacity for the situation of no-flow at different inlet fluid temperatures is the same as equation (6) with the flow rate per absorber area (G) equal to zero.

$$C_c = \frac{(F'U_L)(t_2 - t_1)}{\ln\left[\frac{T_o(t_1) - T_a}{T_o(t_2) - T_a}\right]} \tag{7}$$

The transient performance data of the two glass selective surface collector was plotted in the manner of equation (6). The correlations of the transient test data for flow and no-flow of the collector fluid are given in figure 6. In the case of flow through the collector a linear correlating curve was obtained over the full range of the transient condition. For no-flow a linear curve was not obtained until six (6) minutes had elapsed. The no-flow case is complicated by transient fluid natural convection effects and this could be one of the factors that would account for the initial nonlinear correlation.

According to equation (6) the collector heat capacity may be calculated from the slopes of the curves of figure 6. The resulting collector heat capacities for flow and no-flow are given in table I. The differences noted in table I are to be expected since the collector heat capacity equation (eq. (6)) derived in reference 3 combines the heat capacities of the individual collector components (glass, metal, insulation, liquid, etc.) into one overall heat capacity. It is to be expected that the temperature response of the individual components will be different for flow versus no-flow.

Use of Mirror Boosters

An energy balance for a collector with the reflector configuration of figures 1(b) and 7 results in the following performance equation, as derived in appendix A.

$$\eta = F_R(\alpha\tau)_{\theta_i=0} Z - \frac{W}{\lambda} F_R U_L \frac{(T_1 - T_a)}{I_{dr}} \tag{8}$$

where

$$Z = \frac{W}{\lambda} + \left(1 - \frac{W}{\lambda}\right) \overline{\rho} \frac{(\alpha\tau)_{\theta_i=(\pi/2)-\psi}}{(\alpha\tau)_{\theta_i=0}}$$

and

$$\frac{(\alpha\tau)_{\theta_i=(\pi/2)-\psi}}{(\alpha\tau)_{\theta_i=0}} = 1.0 + b_0\left[\frac{1}{\cos\left(\frac{\pi}{2} - \psi\right)} - 1.0\right]$$

In the derivations of equation (8) it was assumed that all the radiation which leaves the side reflectors reaches the collector. In the test conducted with the simulator the side reflectors were set up so as to permit the above condition. The pertinent geometric values for the collector tested were as follows:

$$\frac{\lambda}{W} = 2.12$$

$$\phi = 62^\circ$$

$$\psi = 2\phi - \pi/2 = 34^\circ$$

As indicated above, the geometric concentration ration (λ/W) for the collector-mirror system was 2.12.

A comparison of the performance equation for a collector with reflectors (eq. (8)) with the performance equation for a collector with no reflectors gives the following differences:

Collector without reflectors	Collector with reflectors
$Z = 1$	$Z < 1$
$\frac{W}{\lambda} = 1$	$\frac{W}{\lambda} < 1$

The above comparison shows that the use of reflectors should result in a lowering of efficiency for conditions of relatively low inlet temperature and/or high radiation. At these conditions the left side of equation (8) dominates the collector efficiency, and is lower for a collector with reflectors ($Z < 1$) than for a collector without reflectors ($Z = 1$). The reason for this is that in the use of reflectors to collect and redirect solar radiation, there is a reflection loss (~15% or more) at the mirror reflector surface and an additional radiation loss (~11%) at the collector due to the increased angle of radiation incidence created by the reflectors.

Since the right side of equation (8) dictates the decrease in efficiency with increased fluid temperature, the use of reflectors should result in increased efficiency at the fluid temperatures (~200° F) required for solar air conditioning. The use of reflectors causes an effective decrease in the heat loss quantity $[(W/\lambda)F_R U_L]$ of the performance equation, and thereby diminishes the effect that heat loss has on collector efficiency.

Figure 8 shows the experimental results and the predicted performance (eq. (8)). The performance curve for the collector having no reflector is also shown in figure 8 so as to demonstrate the effect of the reflectors on collector efficiency. The overall effect of the reflectors is indeed to lower collector efficiency, below the temperature-flux range $\left(\frac{T_1 - T_a}{I_{dr}} > 0.35\right)$ encountered in solar a.c. applications. However, for those conditions requiring maximum utilization of solar cooling, the use of mirror boosters could increase collector efficiency by as much as 30 percent at $T_1 = 200°$ F, $T_a = 80°$ F, and $I_{dr} = 250$ Btu/hr ft^2.

Also shown in figure 8 is the analytical prediction for efficiency of the collector with side mirror reflectors. This prediction from equation (8) was made by using the collector performance parameter ($F_R\alpha\tau$ and $F_R U_L$) of the collector without reflectors; and a mirror reflectivity of 0.85 for the purpose of calculating collector performance with equation (8). The analytical prediction is higher than the experimental correlation and this is probably due to the reflective component of radiation from the mirror not being exactly specified. Using equation (8) and the experimental value of the correlation intercept from figure 8, a calculation was made for average reflectivity ($\bar{\rho}$). The value of the calculated reflectivity is 0.62. The calculated reflectivity is lower than one would expect, indicating the presence of additional reflective losses which were not accounted for in the energy balance used to derive equation (8). This unaccounted reflective loss is probably due at least in part to the imperfect collimation of the simulator which allows some of the reflecting rays of radiation to miss the plane of the collector. This effect could be especially pronounced along the edges of the reflecting mirror. This difference between experiment with the simulator and analysis suggests that this collector with side reflectors would have slightly better performance under actual sunlight conditions.

The advantage of the use of mirror reflectors is more easily seen by observing how much additional energy is collected with reflectors and the corresponding cost. A comparison of the useful energy collected with and without reflectors is given by the following equation that is based on the derivation of appendix A.

$$\frac{Q_{u,r}}{Q_u} = \frac{F_R(\alpha\tau)_{\theta_{i=0}} Z' - F_R U_L \dfrac{(T_1 - T_a)}{I_{dr}}}{F_R(\alpha\tau)_{\theta_i=0} - F_R U_L \dfrac{(T_1 - T_a)}{I_{dr}}} \tag{9}$$

where

$$Z' = 1 + \left(\frac{\lambda}{W} - 1\right)\overline{\rho}\,\frac{(\alpha\tau)_{\theta_i=(\pi/2)-\psi}}{(\alpha\tau)_{\theta_i=0}}$$

The values of $F_R(\alpha\tau)_{\theta_{i=0}}$ and $F_R U_L$ are determined from the intercept and slope of figure 3.

A plot of equation (9) is given in figure 9. Figure 9 demonstrates, as expected, the increase in useful energy due to the mirror reflectors. This increase is important to overcome the heat loss encountered at temperatures required for solar air conditioning. This effect was mentioned above in terms of the collector efficiency curves of figure 8. However, the additional energy collected by the mirror reflectors needs to be justified in terms of a decrease cost per energy collected by the entire collector system.

Present cost figures indicate that the collector cost is about three times the reflector cost, for the particular collector-reflector combination of this study. Using this value, and the results of figure 9, permits a relative cost of energy comparison for a collector with and without reflectors for a solar radiation incident angle of zero.

The energy cost comparison shown in figure 10 demonstrates the potential of reflectors to decrease the overall cost of collecting solar energy for high temperature applications like solar cooling. This cost reduction becomes especially significant at the higher fluid temperatures required for air conditioning, since such high temperature collectors are relatively expensive.

CONCLUSIONS

A flat plate collector with two glass covers and an absorber with a selective surface was given extensive performance tests in a solar simu-

lator facility. These tests give a detailed description of collector performance under different conditions of solar radiation flux, solar incidence angle, fluid inlet temperature, and fluid flow rate. The results of the tests are summarized as follows:

1. Correlation of the efficiency data according to the Hottel-Whillier equations was found to be applicable over a wide range of radiation flux values (70 to 300 Btu/hr ft^2).

2. The effect of flow rate on collector performance was consistent with analytical prediction.

3. The transient behavior of the collector as measured by an overall heat capacity was found to differ slightly for the two situations of flow and of no-flow of the collector coolant.

4. The use of side reflectors to boost the solar flux for a solar incident angle of zero increases collector efficiency by approximately 30 percent at the high-temperature conditions required for solar air conditioning. This performance increase can be predicted by using the performance correlation of the collector without reflectors, modified as to take into account the additional geometric effect on heat flux created by the reflectors.

SYMBOLS

A_a absorber areas, ft^2

C_c collector heat capacity, Btu/hr-ft^2, ^oF

C_p fluid heat capacity, Btu/lb, ^oF

F' collector plate efficiency factor, dimensionless

F_R collector plate heat-removal efficiency, dimensionless

G flow rate of collector fluid, lb/hr-sq ft of absorber surface

h_f heat transfer coefficient, Btu/hr ft^2, ^oF

$K_{\alpha\tau}$ incident angle modifier, dimensionless

I_{dr} incident direct solar radiation, Btu/hr-ft^2 (in collector plane)

L collector length, ft

$\dot{m}$ flow rate, lb/hr

Q rate of thermal energy, Btu/hr

T_a ambient temperature, ^oF

T_o fluid outlet temperature, ^oF

T_p collector plate temperature, ^oF

T_1 fluid inlet temperature, ^oF

$\overline{T}_f$ average collector fluid temperature, ^oF

t time, hr

U_L overall collector heat loss coefficient, Btu/hr-ft^2, ^oF

W collector width, ft

α collector surface absorptance, dimensionless

η collector efficiency, dimensionless

θ_i solar incident angle, deg

λ maximum width of reflector opening, ft

ρ reflectivity, dimensionless

τ effective transmittance

Superscript:

$\overline{\ }$ average conditions

Subscripts:

A absorbed

i incident

L loss

r with reflectors

u useful

APPENDIX - DERIVATION OF COLLECTOR PERFORMANCE EQUATION WHEN SIDE REFLECTORS ARE USED

The heat balance for the collector model shown in figure 7 is as follows:

$$Q_u = Q_A - Q_L \tag{A1}$$

The energy absorbed by the collector is determined as a sum of the solar energy which reaches the collector directly and the solar energy which reaches the collector via the mirror reflectors. It is assumed that the reflectors are positioned so that all of the radiation energy which impinges on the reflectors reaches the collector surface. The equation for the absorbed energy is as follows:

$$Q_A = I_{dr}(\alpha\tau)_{\theta_i=0}WL + I_{dr}(\lambda - W)L\bar{\rho}(\alpha\tau)_{\theta_i=(\pi/2)-\psi} \tag{A2}$$

The energy loss is comprised of that energy which leaves the collector by convection and by radiation. This energy loss is expressed as follows:

$$Q_L = A_a U_L(\bar{T}_p - T_a) \tag{A3}$$

Combining equations (A1), (A2), and (A3) and defining collector efficiency as

$$\eta = \frac{Q_u}{Q_i} = \frac{Q_u}{I_{dr}\lambda L} \tag{A4}$$

we have the following performance equation:

$$\eta = \frac{W}{\lambda}(\alpha\tau)_{\theta_i=0} + \left(1 - \frac{W}{\lambda}\right)\bar{\rho}(\alpha\tau)_{\theta_i=(\pi/2)-\psi} - \frac{A_a}{\lambda L}\frac{U_L(\bar{T}_p - T_a)}{I_{dr}} \tag{A5}$$

Assuming that the collector absorber area is equal to the aperture area for receiving sunlight ($A_a = WL$) and using the approach of references 7 and 8 to express the average plate temperature in terms of the fluid inlet temperatures (T_1) and a flow factor (F_R), equation (A5) can be written as follows:

$$\eta = F_R\left[\frac{W}{\lambda} + \left(1 - \frac{W}{\lambda}\right)\bar{\rho}\frac{(\alpha\tau)_{\theta_i=(\pi/2)-\psi}}{(\alpha\tau)_{\theta_i=0}}\right](\alpha\tau)_{\theta_i=0} - \frac{W}{\lambda}\frac{U_L(T_1 - T_a)}{I_{dr}} \tag{A6}$$

REFERENCES

1. F. F. Simon and P. Harlamert, Flat-Plate Collector Performance Evaluation. The Case for a Solar Simulation Approach. NASA TM X-71427 (1973).

2. K. Yass and H. B. Curtis, Low-Cost, Air Mass 2 Solar Simulator, NASA TM X-3059 (1974).

3. F. F. Simon, Flat-Plate Collector Performance Evaluation with a Solar Simulator as a Basis for Collector Selection and Performance Prediction, NASA TM X-71793 (1975).

4. H. C. Hottel and B. B. Woertz, The Performance of Flat-Plate Solar-Heat Collectors. ASME Transactions, 64, 91 (1942).

5. H. C. Hottel and A. Whillier, "Evaluation of Flat-Plate Collector Performance," Transactions of the Conference on the Use of Solar Energy. Vol. 2, Pt. 1, University of Arizona Press, p. 74 (1958).

6. J. W. Ramsey, J. T. Borzoni, and T. H. Holland, Development of Flat Plate Solar Collectors for the Heating and Cooling of Buildings. Rept. 2852-40057, Honeywell, Inc. (June 1975); also NASA CR-134804.

7. R. W. Bliss, Jr., The Derivation of Several "Plate-Efficiency Factors" Useful in the Design of Flat-Plate Solar Collectors. Sol. Energy, 3, 55 (1959).

8. F. F. Simon and E. H. Buyco, Outdoor Flat-Plate Collector Performance Prediction from Solar Simulator Test Data. AIAA Paper No. 75-741, Denver, Colorado, (1975).

TABLE I. - EXPERIMENTAL COLLECTOR HEAT CAPACITY

G, lb/hr-ft^2	C_c, Btu/hr-ft^2 $^\circ$F $^\circ$F
10	0.7
0	.9

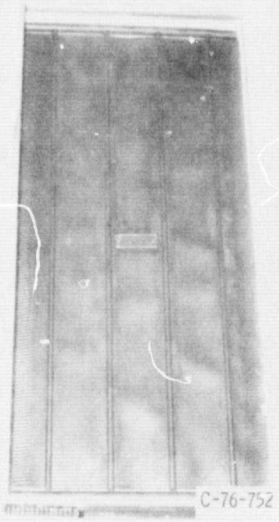

(a) TESTED COLLECTOR.

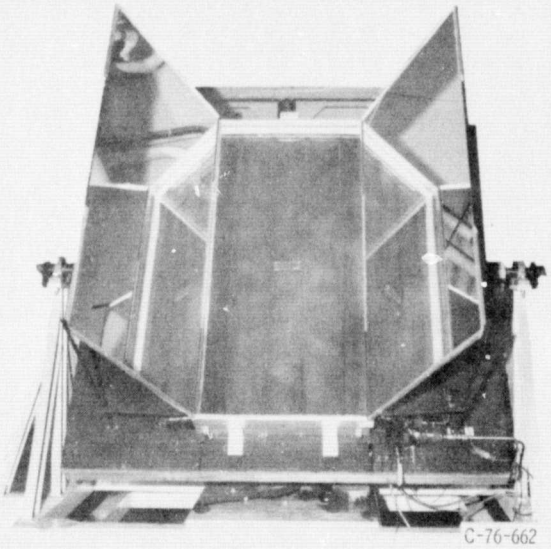

(b) COLLECTOR WITH SIDE REFLECTORS.

Figure 1. - Collectors.

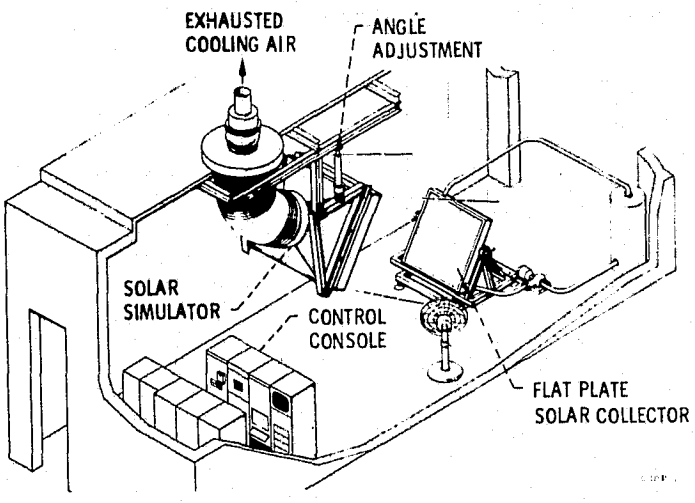

Figure 2. - Indoor test facility.

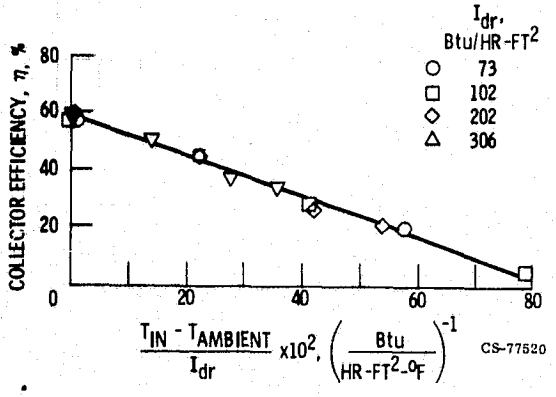

Figure 3. - Collector efficiency (η) as a function of inlet temperature (T_{in}) and incident flux (I_{dr}) (G = 10 lb/hr-ft^2; θ_i = 0).

E-7959

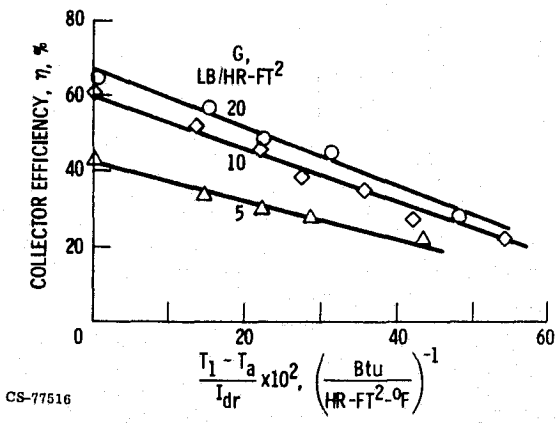

Figure 4. - Collector efficiency as a function of inlet temperature, incident flux, and flow rate ($\theta_i = 0$).

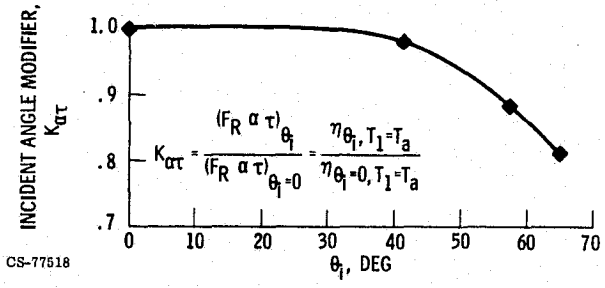

Figure 5a. - Variation of incident angle modifier with incident angle.

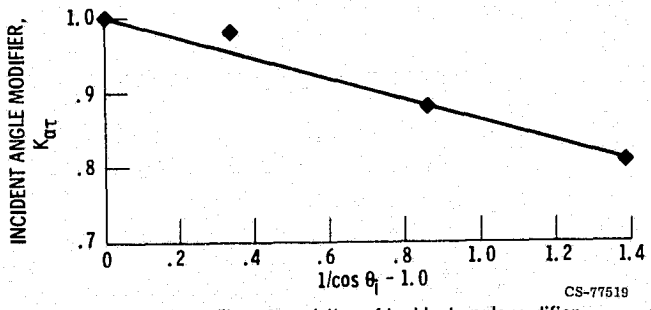

Figure 5b. - Correlation of incident angle modifier.

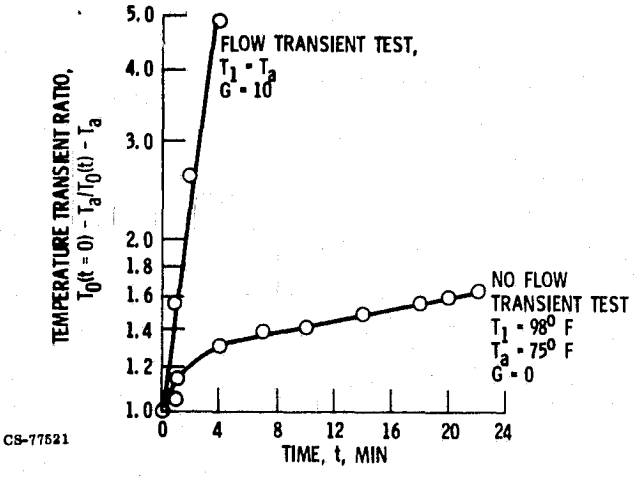

Figure 6. - Thermal transient correlation for flow and no-flow.

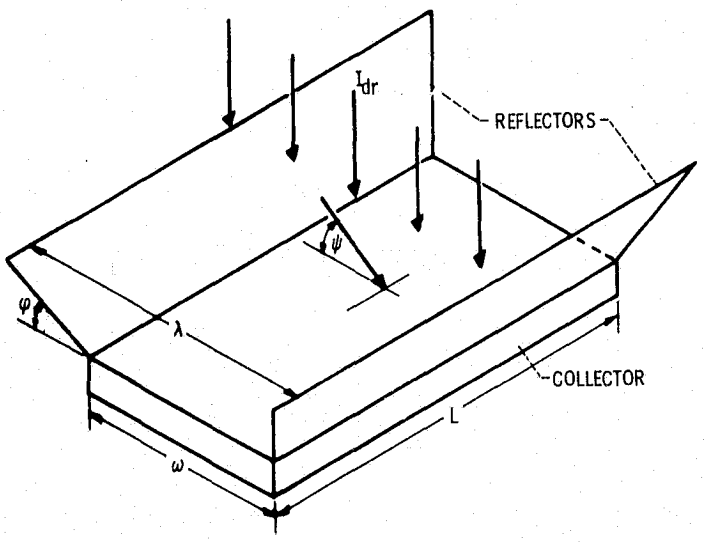

Figure 7. - Model of collector with reflectors.

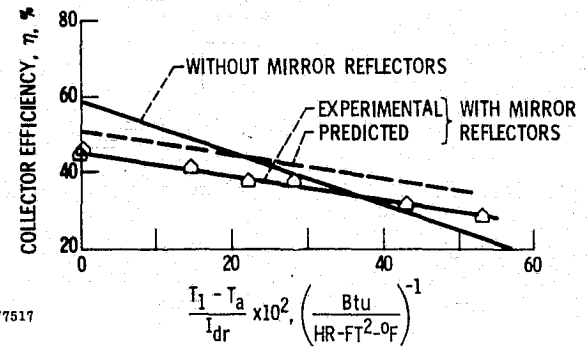

Figure 8. - Effect of side reflectors on collector performance ($G = 10$ lb/hr-ft^2).

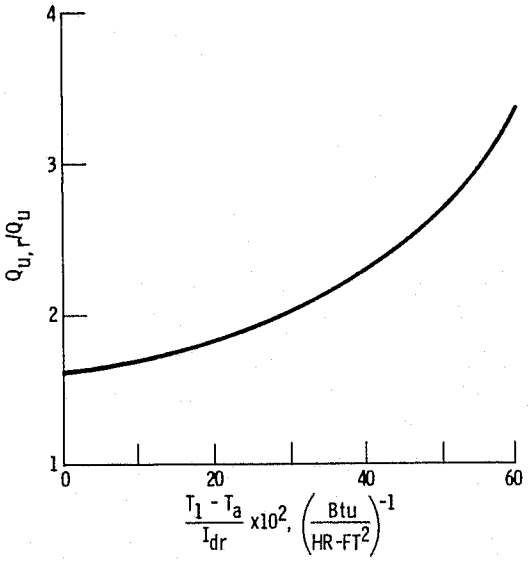

Figure 9. - Effect of side reflectors on the relative increase in useful energy collected.

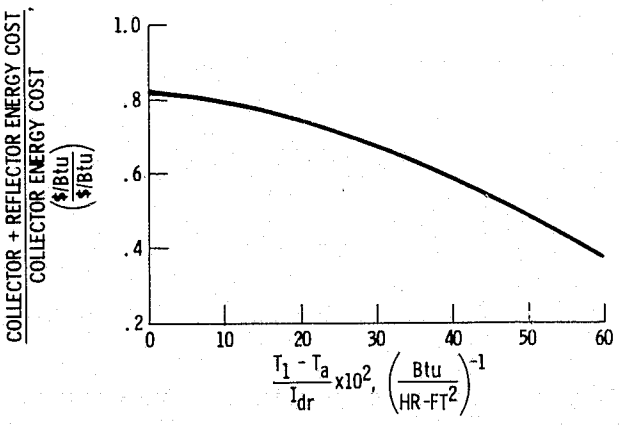

Figure 10. - Relative energy cost for collector with and without collectors ($\theta_i = 0$, $G = 10$ lb/hr-ft^2, collector cost/reflector cost = 3).

E-8959